Multiplexed single-molecule measurements with magnetic tweezers

Noah Ribeck and Omar A. Saleh

Citation: Rev. Sci. Instrum. **79**, 094301 (2008); doi: 10.1063/1.2981687
View online: http://dx.doi.org/10.1063/1.2981687
View Table of Contents: http://aip.scitation.org/toc/rsi/79/9
Published by the American Institute of Physics

Multiplexed single-molecule measurements with magnetic tweezers

Noah Ribeck[1] and Omar A. Saleh[2]
[1]*Physics Department, University of California, Santa Barbara, Santa Barbara, California 93106, USA*
[2]*Materials Department and Biomolecular Science and Engineering Program, University of California, Santa Barbara, Santa Barbara, California 93106, USA*

(Received 21 March 2008; accepted 22 August 2008; published online 15 September 2008)

We present a method for performing multiple single-molecule manipulation experiments in parallel with magnetic tweezers. We use a microscope with a low magnification, and thus a wide field of view, to visualize multiple DNA-tethered paramagnetic beads and apply an optimized image analysis routine to track the three-dimensional position of each bead simultaneously in real time. Force is applied to each bead using an externally applied magnetic field. Since variations in the field parameters are negligible across the field of view, nearly identical manipulation of all visible beads is possible. However, we find that the error in the position measurement is inversely proportional to the microscope's magnification. To mitigate the increased error caused by demagnification, we have developed a strategy based on tracking multiple fixed beads. Our system is capable of simultaneously manipulating and tracking up to 34 DNA-tethered beads at 60 Hz with ~1.5 nm resolution and with ~10% variation in applied force. © *2008 American Institute of Physics.*
[DOI: 10.1063/1.2981687]

I. INTRODUCTION

One advantage of single-molecule (SM) studies on the physics and chemistry of biological molecules is that they are sensitive to heterogeneity in the sample. By building up a histogram of measured characteristics from individual biomolecules, the SM experiment directly estimates the shape of the underlying distribution. This provides more information on the studied system than so-called bulk measurements, in which the experimental output is an average over a large number of molecules, and thus is insensitive to heterogeneity. However, the SM approach can be time consuming: to make a statistically reliable estimate of the distribution, a SM experiment must generate a large amount of data from many biomolecules. SM techniques that generate data one molecule at a time are intrinsically limited in throughput, creating a significant practical hurdle for acquiring the needed data set. SM fluorescence experiments have overcome this hurdle by using multiplexed approaches, in which wide-field imaging is used to track several individual molecules simultaneously.[1,2] In contrast, single-molecule manipulation (SMM) experiments (using devices such as the atomic force microcope,[3] optical tweezers,[4] and magnetic tweezers[5,6]) typically acquire data one molecule at a time.

The logical solution to this problem is to design a method capable of performing multiple SMM experiments in parallel. Here we present such a strategy for magnetic tweezers, which are based on the manipulation of a single DNA molecule tethered on one end to a glass surface and on the other to a superparamagnetic bead.[5,7] The tethered DNA molecule is stretched by subjecting the bead to a magnetic force using an externally applied magnetic field gradient. The bead is imaged in a microscope, and computer analysis of the image gives the bead's three-dimensional position, and thus the end-to-end extension of the DNA.[8] Since magnetic tweezers implement manipulation using a field that is relatively homogeneous over a wide area, they are an ideal candidate for multiplexing. Simultaneously manipulating and measuring multiple bead/DNA complexes with magnetic tweezers presents three challenges:

(1) To achieve consistent, calibrated manipulation of all beads. In a truly parallel SMM experiment, all beads would be manipulated with identical force (in magnitude and direction). In practice, polydispersity in the beads' magnetic properties makes identical forces unattainable. Thus, while nearly identical forces are desirable, the force must be calibrated for each bead individually.
(2) To maintain the data acquisition rate. The computer analysis required to convert the image of a bead to the extension of the tethered DNA molecule is time consuming for the processor. Thus, when attempting to analyze multiple beads simultaneously in real time, it is important to ensure that the image analysis does not slow the data acquisition rate.
(3) To maintain experimental accuracy. Visualizing multiple beads simultaneously is aided by decreasing the microscope magnification and thus enlarging the field of view. Demagnification is limited by the need to maintain an image resolution high enough to accurately compute the bead position.

We address each of these challenges and demonstrate a system of multiplexed magnetic tweezers capable of simultaneously manipulating 34 tethered beads with forces known for each bead and varying by ~10% across the population while measuring their positions at 60 Hz with nanometer-scale accuracy. We also discuss strategies for using multiplexing to minimize experimental noise.

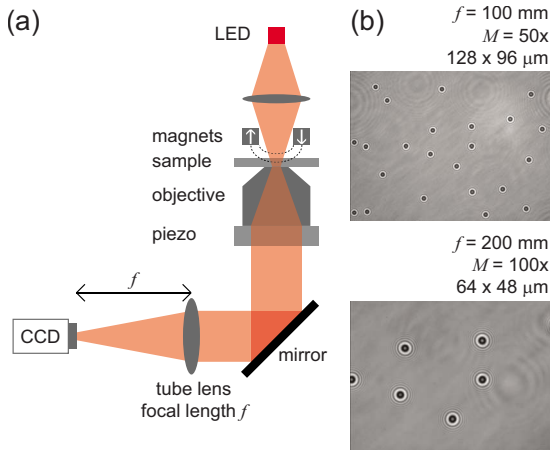

FIG. 1. (Color online) (a) Schematic of the magnetic tweezers and inverted microscope. Magnification M is controlled by varying the focal length f of the tube lens and maintaining the camera a distance f behind the lens. The 100× objective has a reference focal length of 200 mm, so $M=f/(2\ \text{mm})$. (b) Images of 1 μm magnetic beads using different values of f, with M and the size of the field of view noted.

II. METHODS AND MATERIALS

All experiments are performed using a custom-built inverted microscope illuminated by a 650 nm light emitting diode with 7 nm spectral width (Roithner Lasertechnik PR65-F1P0T). The microscope consists of a 100× oil-immersion objective (Nikon CFI Plan Achromat, numerical aperture (NA)=1.25), set into a piezoelectric stage (Physik Instrumente P-725) for nanopositioning of the focal plane, and a tube lens that forms an image captured at a 60 Hz frame rate by a 782×582 pixel (8.37 μm pixel spacing) charge coupled device camera (JAI CV-A10 CL). As shown in Fig. 1, both the position of the camera behind the tube lens and the focal length of the lens are variable, allowing us to adjust the magnification of the microscope (and consequently the extent of the field of view). The applied magnetic field is generated by a pair of permanent rare-earth (NdFeB) magnets (12.5 mm cubes, DuraMag NS-505050) located above the sample stage, separated by 1 mm, and with their magnetic moments aligned antiparallel to each other. Variation of the field in the sample plane is achieved by vertically translating the magnets with a dc servo motor (Physik Instrumente M-126.PD1) between 1 and 20 mm from the sample plane.

DNA samples are generated by polymerase chain reaction (PCR) from a 5386 base pair (bp) section of the Lambda-phage genome (New England Biolabs N3011) using one biotinylated primer and one digoxigenin-labeled primer (Integrated DNA Technologies). Bead/DNA tethers are formed as described[8] within a flow cell that consists of two cover glasses joined by a double sided tape. The flow cell is passivated with a solution of 0.1% Tween 20 (Sigma-Aldrich P9416) and 0.1% Pluronic F-127 (Sigma-Aldrich P2443) for 10 min prior to the addition of magnetic beads. Typical choices for tethered paramagnetic beads are Dynal MyOne (1 μm diameter, Invitrogen 650-01) and Dynal M280 (2.8 μm diameter, Invitrogen 112-05D).

Once bead/DNA tethers are formed, the bead position (x,y,z) versus time is measured in real time using an image analysis routine written in LABVIEW (National Instruments), similar to that developed by Gosse and Croquette.[8] To track the bead position in x and y (i.e., lateral position within the image), we measure from a single frame the intensity versus pixel position $I(x)$ of a set of pixels running in the x direction through the bead center from the previous frame. The maximum of the self-convolution of $I(x)$ gives the shift of the bead center in x from the previous to the current image. An identical calculation is carried out in y. The number of pixels used to define $I(x)$ is defined as the window size; typically, we use window sizes between 64 and 128 pixels. For tracking bead position in z (the vertical direction), we utilize the increase in radii of the bead's diffraction rings as the bead moves away from the focal plane. The observed radii of the diffraction rings are compared to calibration data obtained by moving the focal plane in known increments while the tethered bead is held stationary. Additionally, we track a reference bead that is continuously fixed to the surface; typically, this reference is a polystyrene bead with a diameter of 1 μm (Bangs Laboratories PS04N) or 2.5 μm (Bangs Laboratories PS05N). The calculated position of the fixed (reference) bead is subtracted from the calculated position of the tethered (experimental) bead, which eliminates common mode noise arising from mechanical drift, thermal drift, or vibration in the apparatus.

III. EXPERIMENTAL DESIGN AND DATA ACQUISITION

A. Consistent manipulation of each tethered bead

Performing parallel manipulation experiments requires each tethered bead to be subjected to an approximately identical force. The force $\vec{F}$ applied to a bead is given by $\vec{F}=[\vec{m}(\vec{B})\cdot\vec{\nabla}]\vec{B}$, where $\vec{B}$ is the applied magnetic field, and $\vec{m}(\vec{B})$ is the field-dependent magnetic moment of the paramagnetic bead. Thus, applying identical forces to all beads requires an identical field gradient in the vicinity of each bead and for each bead to have the same moment. Since the beads are paramagnetic, the constraint on moment requires the field strength to be identical near each bead.

In practice, the constraints on the magnetic field parameters (strength and gradient) are not difficult to achieve. At 50× magnification, the field of view of the microscope is $128\times96\ \mu\text{m}^2$, which is much smaller than all relevant length scales of the magnets. To confirm that the magnetic field parameters are constant over the space accessible to the beads, we performed finite-element calculations of the field with the magnets located 1 mm from the sample plane. We found that from the center to the edge of the field of view, the magnitude of the field strength varies by no more than 0.02%, and the magnitude of the gradient varies by no more than 0.2%. The direction of the field gradient is also quite constant: the lateral component of the field gradient is no more than 1.5% of the vertical component at the edge of the field of view.

In contrast to the magnetic field, it is difficult to control the magnetic properties of the beads themselves due to their intrinsic polydispersity in size. The magnetic beads we use here (Dynal MyOne) have a mean diameter of 1.05 μm with

a relative variation in diameter of 3%. Basic magnetostatics predicts that the bead's magnetic moment increases linearly with particle volume; thus, a 3% variation in diameter leads to a 9% variation in magnetic moment, greatly exceeding the variation in magnetic field parameters. Since polydispersity in bead magnetic moments is unavoidable, it is necessary to calibrate the force applied to each bead individually. This is done by measuring the Brownian trajectory of each tethered bead and applying a power spectrum-based analysis.[9] Our measurements indicate that the applied force typically varies by 7%–10% when simultaneously manipulating multiple beads. This variation is consistent with polydispersity in bead size being the limiting factor in applying consistent forces. However, since the force can be measured for each individual bead, this variation is acceptable.

B. Maintaining the data acquisition rate

Tracking the tethered bead position in real time provides several experimental advantages. Notably, it facilitates fine-tuning of the experiment while in progress and simplifies postexperiment data analysis. However, real-time tracking is a challenge for multiplexed experiments since the time-consuming image analysis algorithm must be applied to all beads, and all calculations must be completed faster than the frame rate of the camera. Using our tracking algorithm written in LABVIEW on a computer with a 3 GHz processor running Windows XP, each call to the tracking routine takes approximately 1 ms for a single bead when using a window size of 64 pixels. Thus, a serial multiplexed bead tracking routine would be limited to a maximum of ~16 beads, given our camera's 60 Hz frame rate (~16.7 ms per frame). However, LABVIEW allows the code to be multithreaded, meaning that multiple operations within a single program can be subdivided into threads that can be executed in parallel if the computer contains multiple processors. We optimized our tracking code to utilize multithreading on a four-processor computer (i.e., two dual-core processors). This accelerated the computation, allowing for tracking of up to 36 beads simultaneously at 60 Hz.

IV. OPTIMIZATION

A. Limitations on packing density

Optimizing the multiplexed magnetic tweezers involves tracking as many beads as possible. One limit on the number of trackable beads is set by the time constraints of the image analysis routine, as discussed above. A second constraint is the limitation on packing density of the beads themselves: closely spaced magnetic beads can (1) have overlapping diffraction images that affect the image analysis routine and can exert forces on each other through either (2) magnetic dipole or (3) hydrodynamic interactions. We can estimate the minimum allowable spacing from each effect: (1) We have found that the high intensity of the innermost interference ring dominates both the lateral (x,y) and vertical (z) tracking algorithms, so tracking accuracy is not measurably affected by higher-order ring overlap. However, once the innermost rings overlap, the diffraction pattern is no longer sufficiently symmetric, and tracking ability is lost completely. In practice, this requires a spacing of ~5–8 μm between 1 μm diameter beads tethered by DNA ~2 μm in length. Longer tethers require calibration data with a greater amount of defocus, necessitating a greater spacing to ensure no overlap of the innermost ring. (2) According to the manufacturer, Dynal MyOne beads have a mean induced magnetic moment density of 42 emu/cm^3 at saturating magnetic field strength ($|B|>0.5$ T). For these beads, the maximum possible dipole-dipole force is negligible ($|F|<0.1$ pN) for $r>8$ μm. (3) The motion of a bead in solution creates a fluid flow that tends to entrain nearby beads in its wake, causing unwanted correlations between bead trajectories. The strength of this interaction is described by a coupling parameter, ε.[10] In bulk solution, for two beads with radius a separated by a distance r, $\varepsilon \approx (3/2)(a/r)$.[11,12] In our geometry, all beads are located a distance $h<r$ from a glass surface. The presence of this surface screens the hydrodynamic interactions, reducing the coupling constant to $\varepsilon \approx 9(ah^2/r^3)$.[12] For beads spaced as closely as allowed by the other constraints ($r=8$ μm), this screening effect makes the hydrodynamic coupling negligible: for $a=0.5$ μm and $h=2$ μm, $\varepsilon \approx 0.04 \ll 1$. We estimate that such a small value of ε will lead to at most an ~0.1% error in the measurement of applied force.

Thus, a minimal bead-bead separation of ~8 μm for 1 μm beads tethered to ~2 μm DNA permits effective tracking and ensures that interactions between neighboring beads are insignificant. Since the packing density is limited by this minimum spacing, optimization of the multiplexed magnetic tweezers can be accomplished by increasing the microscope's field of view by decreasing the magnification. For N_{total} randomly placed tethers in a field of view with area A, Poisson statistics indicate that the average number satisfying the required minimum distance r from its nearest neighbor is $\langle N_{\text{spaced}} \rangle = N_{\text{total}} \exp(-N_{\text{total}} \pi r^2/A)$. With magnification reduced to 50× (128×96 μm^2 field of view) and a required spacing of $r=8$ μm, this corresponds to a maximum of $\langle N_{\text{spaced}} \rangle = 22$ at $N_{\text{total}}=61$.

This value serves as a rough estimate of the number of beads that can be tracked simultaneously under the aforementioned conditions. However, since we are free to choose an optimal field of view, it is possible to find a field containing more than $\langle N_{\text{spaced}} \rangle$ well-spaced beads. Alternatively, existing technologies for micropatterning of surface-immobilized biomolecules[13] could theoretically be used to create a densely packed array of tethers. This would provide up to 192 well-spaced, trackable tethered beads in a single field of view at 50× magnification provided future improvements in computation speed.

B. Effects of demagnification on bead tracking accuracy

We examined how reducing the magnification affects the accuracy of the bead tracking routine. We prepared flow cells with several bead types (1 μm paramagnetic, 2.8 μm paramagnetic, 1 μm polystyrene, 2.5 μm polystyrene) fixed to

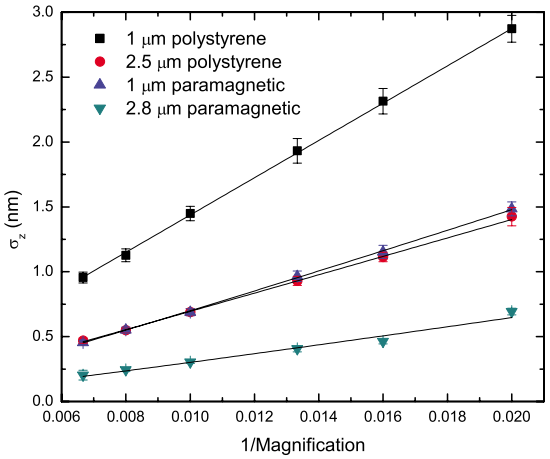

FIG. 2. (Color online) Standard deviation of measured z position of different bead types plotted vs inverse magnification. The solid lines are linear fits to the data of each bead type. All beads are fixed to the glass surface, and each measurement is made using a single reference bead of the same type. Tracking accuracy improves with larger and/or paramagnetic beads likely because such particles scatter more light, enhancing the diffraction pattern.

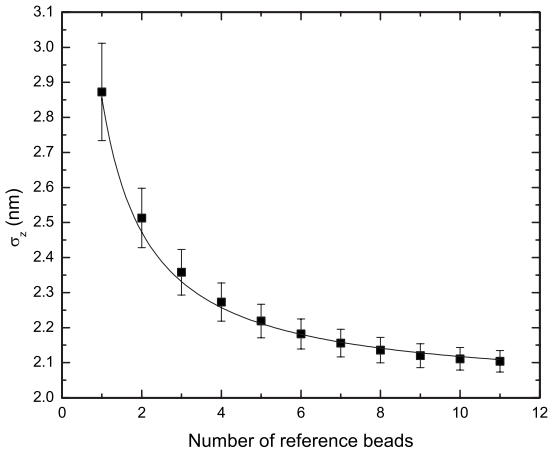

FIG. 3. Standard deviation of the z position of a 1 μm polystyrene bead measured with respect to a varying number N of reference beads of the same type. All beads are fixed to the glass surface, and measurements are made at 50× magnification. The curve is a fit to Eq. (1) with fit parameter $\sigma_0 = 2.019 +/- 0.003$ nm.

the surface and measured the standard deviation in measured position at different magnifications. To fix the beads to the surface, a dilute solution was pipetted onto a glass cover slip and the beads were allowed to sediment and bind nonspecifically to the glass. The water was then air blown off the glass and the cover slip was heated on a hot plate (150 °C for 5 min for the polystyrene beads, 200 °C for 30 min for the magnetic beads). Fixing the beads ensures that any measured deviation in position arises from noise in the tracking routine and not from actual motion of the beads themselves.[14] We tracked the fixed beads at various magnifications while holding constant the background intensity per pixel and the ratio of magnification to window size.[15] The beads were tracked for 3 min (10 800 frames), and the z position of each bead in each frame was subtracted from the position of an arbitrarily chosen reference bead of the same type. We then calculated the standard deviation in z for each bead across the entire acquisition and found that it is inversely proportional to the magnification between 50× and 150× (Fig. 2). While our setup cannot access magnification lower than 50×, we would expect this relation to hold to lower magnifications until the diffraction rings are no longer resolved.

C. A multiplexing-based strategy for noise reduction

We measured bead position in reference to a bead fixed to the surface, i.e., we determined the measured height z_{msd} as $z_{\mathrm{msd}} = z_{\mathrm{expt}} - z_{\mathrm{ref}}$, where z_{expt} (z_{ref}) is the height of the experimental (reference) bead. The experimental error σ_z of z_{msd} is $\sigma_z = \sqrt{\sigma_{\mathrm{expt}}^2 + \sigma_{\mathrm{ref}}^2}$, where σ_{expt} (σ_{ref}) is the error in tracking the experimental (reference) bead. The advantage of subtracting the reference bead position is that common mode noise is absent from this expression. However, subtracting the reference position introduces the intrinsic noise σ_{ref} of tracking the reference bead. This added noise can be minimized by tracking multiple reference beads and averaging their positions. Then, the tracking error is decreased to $\sigma_z(N) = \sqrt{\sigma_{\mathrm{expt}}^2 + \sigma_{\mathrm{ref}}^2/N}$, where N is the number of reference beads, and all reference beads are assumed to be identical. If the experimental bead is identical to the reference beads, then $\sigma_{\mathrm{expt}} = \sigma_{\mathrm{ref}} \equiv \sigma_0$, and the tracking error is

$$\sigma_z(N) = \sigma_0 \sqrt{1 + \frac{1}{N}}. \tag{1}$$

Figure 3 shows σ_z of a 1 μm diameter polystyrene bead fixed to the surface and measured in reference to N other fixed beads of the same type. The data are well fitted by Eq. (1).

D. Determining optimal magnification

Figures 2 and 3 demonstrate that our multiplexing strategy creates opposing trends in the experimental noise. Decreasing the magnification increases the number of visible reference beads, which can be used to *reduce* the tracking noise [Fig. 3, Eq. (1)]. However, decreasing the magnification *increases* the tracking noise of each individual bead (Fig. 2), meaning σ_0 in Eq. (1) increases with decreasing magnification. Which trend dominates? Is there an optimal magnification that minimizes tracking noise? Based on the data in Fig. 2, the noise when using a single reference bead $[\sigma_z(N=1) = \sqrt{2}\sigma_0]$ scales inversely with magnification: $\sigma_0 \propto 1/M$. Additionally, at constant bead density, the number N of randomly placed reference beads in the field of view is related to the magnification M by $N \propto 1/M^2$. By inserting these expressions into Eq. (1), we find

$$\sigma_z(M) \propto \sqrt{\frac{1}{M^2} + C}, \tag{2}$$

with constant C, which depends on the density of reference beads in the sample. It is clear from Eq. (2) that tracking noise decreases monotonically with increasing magnification despite the fact that a lower magnification allows for the use of more reference beads. However, even at a low magnification (50×), tracking error on the order of ~1–2 nm is achievable with a single reference bead (Fig. 2). This is an acceptable accuracy for many SM experiments, particularly

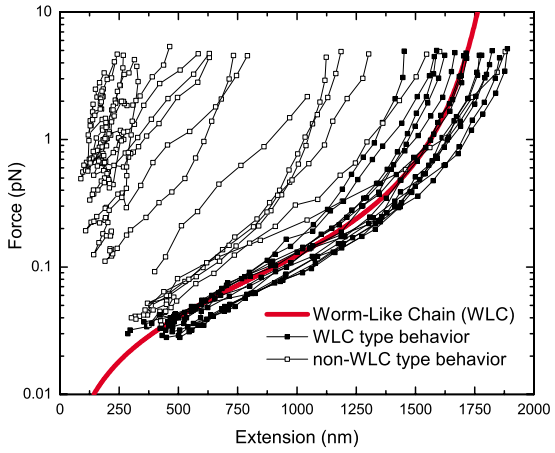

FIG. 4. (Color online) Force-extension curves of 5386 bp DNA molecules tethered to 1 μm magnetic beads. The 34 plotted curves were measured simultaneously at 50× magnification in a solution of 10 mM tris and 1 mM ethylenediaminetetraacetic acid (EDTA), *p*H 7.5. The solid curve shows the expected WLC behavior for a DNA molecule of this length, using a persistence length of 50 nm.

in low-force situations where Brownian motion of the experimental bead, and not tracking error, becomes the dominant noise source. Using this low magnification allows us to take full advantage of our ability to track many tethered beads simultaneously in order to maximize data throughput.

V. DEMONSTRATION

To illustrate the capabilities of the multiplexed magnetic tweezers, we prepared a sample of beads tethered by 5386 bp DNA and measured DNA extension versus applied force for multiple beads. A total of 34 adequately spaced ($r \geq 8$ μm) tethers was chosen, while 10 were ignored due to inadequate spacing.

The beads were tracked using a 64 pixel window size and 50× magnification. The force applied to each bead at each position was calibrated using power spectrum-based analysis of the bead trajectories.[9] We measured force-extension curves for 34 tethered magnetic beads while using 2 reference beads, demonstrating our ability to track up to 36 beads simultaneously (Fig. 4).

Of the 34 tethered beads, 14 force-extension curves showed the wormlike chain (WLC) behavior expected for double-stranded DNA, with persistence lengths ranging between 43 and 54 nm, consistent with prior data in a similar buffer.[16] The remaining beads exhibit a range of force-extension behavior. Some show extensibility reminiscent of the low-force behavior of single-stranded DNA,[17] while others vary only slightly, if at all, with force. These anomalous behaviors are typical in SMM experiments: DNA damage occurring during preparation, handling, or storage could give rise to multiple nicks and/or bare single-stranded regions that give rise to non-WLC force-extension behavior. Further, some beads might be tethered by multiple DNA molecules or be nonspecifically bound to the glass surface. The power of multiplexing is clear in Fig. 4: instead of using a time-consuming search to find a single suitable tether, we can simply track all visible beads simultaneously. The large number tracked ensures that some fraction will exhibit the desired behavior.

VI. CONCLUSION

We have developed magnetic tweezers capable of manipulating multiple bead/DNA complexes simultaneously while measuring the extension of each DNA molecule in real time. We have demonstrated parallel manipulation and measurement of 34 DNA-tethered beads. The manipulation force is calibrated for each bead individually; for different beads manipulated at one time, the force can vary by ~10% due to polydispersity in the beads themselves but not due to variation in magnetic field parameters. We have found that, due to constraints on bead packing density, a wide field of view must be used in order to take full advantage of the increase in data throughput that the multiplexed tracking algorithm provides. We have shown that while the tracking accuracy decreases with demagnification, the resolution is an acceptable ~1–2 nm for magnifications as low as 50× (128 × 96 μm^2 field of view). The wider field of view also allows for averaging over multiple reference beads, which constitutes a novel multiplexing-based strategy for removing extraneous noise from the measurement. Overall, our multiplexed strategy solves all issues associated with the low data throughput of SMM experiments and should find wide application to a variety of questions in the mechanics of DNA and of protein-DNA interactions.

ACKNOWLEDGMENTS

The authors thank T. M. Squires and K. Kim for helpful discussions. This work was supported by start-up finding from the UCSB College of Engineering and College of Letters and Science.

[1] T. Ha, I. Rasnik, W. Cheng, H. P. Babcock, G. H. Gauss, T. M. Lohman, and S. Chu, Nature (London) **419**, 638 (2002).
[2] X. W. Zhuang, L. E. Bartley, H. P. Babcock, R. Russell, T. J. Ha, D. Herschlag, and S. Chu, Science **288**, 2048 (2000).
[3] M. Rief, M. Gautel, F. Oesterhelt, J. M. Fernandez, and H. E. Gaub, Science **276**, 1109 (1997).
[4] K. C. Neuman and S. M. Block, Rev. Sci. Instrum. **75**, 2787 (2004).
[5] T. R. Strick, J. F. Allemand, D. Bensimon, A. Bensimon, and V. Croquette, Science **271**, 1835 (1996).
[6] T. Lionnet, A. Dawid, S. Bigot, F. X. Barre, O. A. Saleh, F. Heslot, J. F. Allemand, D. Bensimon, and V. Croquette, Nucleic Acids Res. **34**, 4232 (2006).
[7] T. R. Strick, J. F. Allemand, D. Bensimon, and V. Croquette, Biophys. J. **74**, 2016 (1998).
[8] C. Gosse and V. Croquette, Biophys. J. **82**, 3314 (2002).
[9] K. Berg-Sorensen and H. Flyvbjerg, Rev. Sci. Instrum. **75**, 594 (2004).
[10] Hydrodynamic coupling is properly described through a diffusivity or mobility tensor that indicates how motion of bead 1 in direction *i* affects the motion of bead 2 in direction *j*. Here, we quote the largest coupling parameter from that tensor (that for bead motion parallel to the bead-bead separation direction). See Ref. 12 for details.
[11] J. C. Meiners and S. R. Quake, Phys. Rev. Lett. **82**, 2211 (1999).
[12] E. R. Dufresne, T. M. Squires, M. P. Brenner, and D. G. Grier, Phys. Rev. Lett. **85**, 3317 (2000).
[13] P. M. Mendes, C. L. Yeung, and J. A. Preece, Nanoscale Res. Lett. **2**, 373 (2007).
[14] We judged successful fixing by measuring the power spectra of the traces in all three dimensions. For nonspecifically stuck beads prior to heating,

the power spectra exhibited a decrease in amplitude with frequency, indicating that the beads were undergoing constrained Brownian motion. After heating, the power spectra amplitudes were constant with frequency, indicating that the beads were well fixed to the surface, leaving only the white noise intrinsic to the measurement.

[15] The effects of varying certain parameters of the microscope and tracking routine were tested. In the range of $50\times-150\times$ magnification, tracking accuracy in z was negligibly affected by the variation of the following parameters: window size (provided the first diffraction ring is entirely included), background intensity above a particular illumination strength, focal position (provided that the focal plane is within the range of calibration), and illumination numerical aperture.

[16] C. Bustamante, J. F. Marko, E. D. Siggia, and S. Smith, Science **265**, 1599 (1994).

[17] M. N. Dessinges, B. Maier, Y. Zhang, M. Peliti, D. Bensimon, and V. Croquette, Phys. Rev. Lett. **89**, 248102 (2002).